Original Article (Clinical Trial)

Taiwan J Ophthalmol 2024;14:59-69

Access this article online

Quick Response Code:

Website:
http://journals.lww.com/TJOP

DOI:
10.4103/tjo.TJO-D-23-00155

Biomechanical changes in keratoconus after customized stromal augmentation

Sana Niazi[1,2], Jorge Alió del Barrio[3], Farideh Doroodgar[1,2*], Azad Sanginabadi[4], Cyrus Alinia[5], Seyed Javad Hashemian[6], Hassan Hashemi[7], Jorge L. Alio[8,9]

[1]Translational Ophthalmology Research Center, Tehran University of Medical Sciences, Tehran, Iran, [2]Negah Aref Ophthalmic Research Center, Shahid Beheshti University of Medical Sciences, Tehran, Iran, [3]Cornea, Cataract and Refractive Surgery Unit, Vissum Corporación, Alicante, Spain, [4]Department of Optometry, Iran University of Medical Sciences, Tehran, Iran, [5]Department of Public Health, School of Public Health, Urmia University of Medical Sciences, Urmia, Iran, [6]Eye Research Center, Five Senses Institute, Rassoul Akram Hospital, Iran University of Medical Sciences, Tehran, Iran, [7]Noor Ophthalmology Research Center, Noor Eye Hospital, Tehran, Iran, [8]Division of Ophthalmology, Universidad Miguel Hernández, Alicante, Spain, [9]Vissum Miranza Alicante, Alicante, Spain

***Address for correspondence:**
Dr. Farideh Doroodgar, No 3. Ketabi St. Shariati Ave. Tehran 1544914599, Iran.
E-mail: f-doroodgar@farabi.tums.ac.ir

Submission: 04-10-2023
Accepted: 01-01-2024
Published: 20-02-2024

Abstract:

PURPOSE: To verify corneal biomechanical changes, poststromal augmentation using myopic small-incision lenticule extraction's (SMILEs) lenticules in advanced keratoconus (KCN) through Corvis ST (Oculus, Wetzlar, Germany).

MATERIALS AND METHODS: A clinical trial enrolled 22 advanced KCN patients. We implanted lenticules exceeding 100 μ according to a nomogram and evaluated biomechanical factors through Corvis ST at 3-, 6-, and 24-month postimplantation. We examined parameters during the first applanation (A1), second applanation (A2), highest concavity (HC)/max concavity events, and Vinciguerra screening parameters, as recently established criteria derived from the ideal blend of diverse biomechanical and ocular factors and formulated through the application of logistic regression. Regression analyses explored relationships with age, mean keratometry value, thickness, sphere, cylinder, and best-corrected visual acuity.

RESULTS: Patients were well matched for age, intraocular pressure, and central corneal thickness (CCT). The mean spherical equivalent decreased from −13.48 ± 2.86 Diopters (D) to −8.59 ± 2.17 D ($P < 0.007$), and mean keratometry decreased from 54.68 ± 2.77 D to 51.95 ± 2.21 D ($P < 0.006$). Significant increases were observed in HC time (HCT), Radius–central curvature radius at the HC state–, peak distance (PD) during HC state, CCT, first applanation time, and stiffness parameter (A1T and SP-A1), whereas HC deformation amplitude, maximum deformation amplitude ratio at 2 mm, Corvis Biomechanical Index (CBI), integrated radius (IR), second applanation deformation amplitude (A2DA), first applanation velocity and deflection amplitude (A1V and A1DeflA) significantly decreased postlenticule implantation. Multivariable regression revealed age positively correlated with SP-A1 ($P = 0.003$) and negatively with HC delta Arc length ($P = 0.007$). Mean K positively correlated with CCT ($P = 0.05$) and negatively with CBI ($P = 0.032$). Best-corrected visual acuity positively correlated with HCT ($P = 0.044$), and the cylinder positively correlated with PD ($P = 0.05$) and CCT ($P = 0.05$) whereas negatively with IR ($P = 0.025$).

CONCLUSIONS: Stromal augmentation using myopic SMILE lenticules induces significant corneal biomechanical changes in KCN.

Keywords:

Cornea, corneal stroma, keratoconus, stromal lenticule, tissue donors, transplantation

Introduction

Keratoconus (KCN) is diagnosed, graded, and managed with different diagnostic criteria and geographic locations.[1,2] Intrastromal corneal rings enhance visual acuity, and corneal collagen cross-linking (CXL) may slow disease development, and it may be modified to keep the cornea under the damage threshold[3] in relation to ultraviolet (UV) power and duration.[4,5]

How to cite this article: Niazi S, del Barrio JA, Doroodgar F, Sanginabadi A, Alinia C, Hashemian SJ, *et al*. Biomechanical changes in keratoconus after customized stromal augmentation. Taiwan J Ophthalmol 2024;14:59-69.

The Corvis ST (Oculus, Wetzlar, Germany) evaluates the biomechanical response of the cornea to air puff-induced deformation.[6,7] The effects of using different surgeries[7] such as corneal cross-linking, intracorneal ring segments,[8] besides sensitivity and specificity biomechanical parameters including Corvis Biomechanical Index (CBI) have been assessed in the monitoring of KCN.[6,9-16] However, this is the first study for the characterization of *in vivo* biomechanical properties induced by stromal augmentation in KCN, using stromal lenticules of myopic small incision lenticule extraction (SMILE) patients.

The SMILE's lenticule implantation new treatment modality is changing the way we deal with patients with an irregular thin cornea.[17] For better evaluation of the implanted lenticules reported in our previous study,[18] we report biomechanical factors for over 2 years of follow-up as our primary objective in the current study.

Materials and Methods

Study population

In this clinical trial study, 22 eyes (8 males and 14 females; mean age 36.13 ± 2.78 [range: 33–42]) with unilaterally advanced KCN were prospectively recruited from June 2018 to July 2023 by an experienced surgeon (FD). All patients were aware of the surgical procedures and risks and provided written informed consent before surgery. Surgery was offered in all cases as a less invasive alternative to corneal transplantation. The study adhered to the tenets of the Declaration of Helsinki (Clinical Trial Registration Number: NCT03890718).

This article has been investigated at the Ophthalmology Research Center-Ethics Committee of Shahid Beheshti University of Medical Sciences: IR.SBMU.ORC.REC.1399.028.

Small incision lenticule extraction donor selection criteria

The proposed cases for SMILE donors were healthy individuals[18] with stable myopia, 8.5 ≤spherical equivalent ≤11 (hence guaranteeing donor lenticule central thickness >100 μm), age ≥20 years, cylindrical error <−1.00 Diopter (D), and best-corrected visual acuity (BCVA) ≥20/25 diopters while having necessary imaging criteria and good biomechanical properties. For donors, all corneal diseases, glaucoma, nystagmus, angle kappa ≥0.4 mm, a history of inflammatory eye diseases, retinal diseases, immunosuppressive therapy or immunodeficiency, serologic evidence infection with hepatitis B virus, human immunodeficiency virus and hepatitis C virus, pregnancy, and breastfeeding were the exclusion criteria.

The included cases as recipients were KCN eyes with corrected distance visual acuity (CDVA) ≤0.4, which was scheduled according to Figure 1 at different depths depending on the thinnest point in pachymetry.[18,19] Recipients with the best-CDVA was 20/160 or worse in the contralateral eye, cataract, glaucoma, a history of inflammatory eye diseases, retinal diseases, past ocular surgery, CXL history, and considerable central scar, pregnancy, and history of dementia and cognitive impairment were excluded from the study because of their inability to approve the consent form and fulfill follow-up after surgery.

The patients recruited were successfully scheduled for immediate (within 4 h) implantation of the extracted lenticule using the VisuMax (Carl Zeiss Meditec, Jena, Germany) SMILE software. Lenticule implantation with a thickness of more than 100 μ according to Figure 1 was performed.[18] The primary outcome measures included the Corvis ST corneal biomechanical factors. Postoperatively, Corvis ST images were compared with parameters obtained as a baseline before implanting the lenticules in eyes with advanced KCN.

Surgical procedure

Individuals diagnosed with high myopia were slated for SMILE utilizing the VisuMax femtosecond laser from Carl Zeiss Meditec as the donor cases. Concurrently, recipient cases involving patients with KCN were scheduled for surgery on the same day. To enhance comparability, cases were meticulously paired preoperatively, ensuring that more patients with high myopia underwent simultaneous surgery with their counterparts diagnosed with advanced KCN. The entirety of the customized SMILE lenticule implantation procedures was conducted by a singular surgeon (FD) under the administration of topical anesthesia.

A 9.5 mm stromal pocket was made with a 500-kHz VisuMax femtosecond laser system, and two small incisions (2–3 mm) were created at locations 150° superotemporal and 330° inferonasal for the right eye of a patient for a right-handed surgeon and vice versa. In the usual configuration, dissection was performed; then, the prepared donor lenticule was implanted into the space using Kelman forceps. For each case, a saved lenticule was configured for potential utilization in the event of complications.[20] Optisol, as a feasible and useful medium for storage, was used for lenticule storage for 14 days.[21,22] If the donor lenticule was not used within 4 h, it could be sealed in the Optisol GS™ of the Central Eye Bank of Iran.[23] All lenticules were implanted without any intraoperative complications.

A corneal pocket is necessary for lenticule implantation, but it is not present in the VisuMax system. Thus, we had to choose an Intracorneal ring (ICR) plan while applying inner diameter formation at zero to take advantage of VisueMax FSL to create the lenticule in the donor cornea with the intrastromal pocket shaping and fresh lenticule implantation simultaneously. The center of the donor lenticules was S shape marked.[24] In recipients (keratoconic eyes), the center of the pupil and between the corneal and pupillary center in large-angle kappa were considered.

Advanced lenticule forceps (Geuder GmbH) were used to remove the lenticule from the donor eye, which was then handled with advanced Chansue dissectors. Then, using biopsy punches ranging from 3 to 5 mm, it was shaped into a necklace and ring 120° forms [Figure 2]. A punching Kai biopsy punch (Kai Industries Co., Ltd) with a piston allows for accurate biopsy and precision tissue cutting with minimal tissue damage and is available in sizes ranging from 1 to 8 mm (with a 0.50-mm step). Using Kelman forceps to hold the donor lenticule lengthwise along a diameter, the prepared donor lenticule was inserted into the space provided by the upper interface through the small incision. The donor lenticule was distended until it was flat and centered on the corneal vertex, parallel to the fixation axis. The central edge of the lenticule was aligned with the pupillary edge of the recipient cornea during insertion [Figure 2]. In the case of compound forms, the necklace form part was inserted first, followed by the ring 120° part. With the refractive cut anterior and the planar cut posterior, the lenticule's orientation was maintained throughout.

Postoperatively, levofloxacin 0.5% eye drop (Oftaquix, Santen, Tampere, Finland) was applied 4 times a day together with topical prednisolone acetate 1% eye drops 6 times a day for 2 weeks. Topical corticosteroids were tapered after 2 months. Artificial tears were applied every 4 h for 3 months. The patients were examined at 1 d, 2 weeks, 1, 3, 6, 12, and 24 months postoperatively. We did not keep repeating the examination from 1 day to 2 years repeatedly.

Measurements

An autorefractometer (Canon R-50; Canon Inc., Tokyo, Japan) and Pentacam HR (Oculus Optikgerate GmbH,

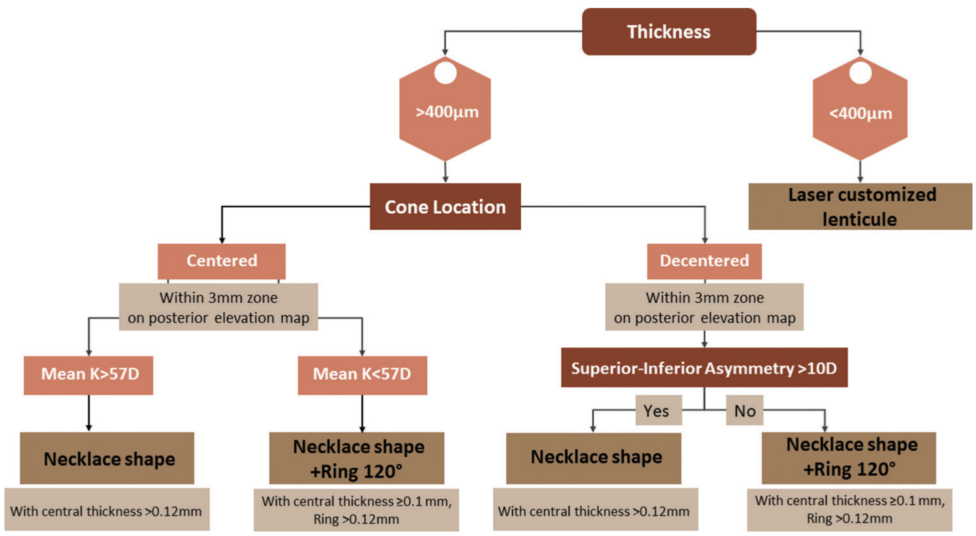

Figure 1: Nomogram of first-stage treatment for advanced keratoconus using stromal donor lenticules during myopic small incision lenticule extraction surgery. D = Diopters

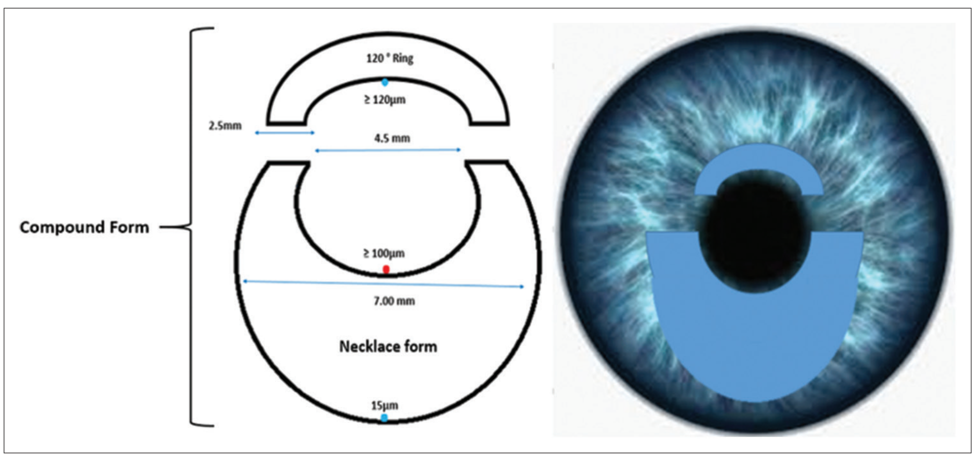

Figure 2: Form of lenticule

Wetzlar, Germany) were used to measure refraction and keratometry measurements, respectively. The Corvis ST measurements and records the corneal biomechanical response to an air-puff at the moment of the first applanation, second applanation, highest concavity (HC) events, and Vinciguerra screening parameters [Table 1].[25]

The current study aimed to record the biomechanical differences between the before the procedure and three follow-up courses after lenticule implantation by Corvis ST [Figure 3]. We used as the biomechanical test only Corvis ST tests with an "OK" rating score in the study. In addition, to ensure the accuracy of each examination, a second manual, a frame-by-frame review of the trial, created by an impartial masked investigator, was performed. Blinking mistakes were excluded from the analysis.

Statistical analyses

We used the mean and standard deviation (SD) for continuous variables and the median and range to present the data. The Pearson correlation coefficient was used as a univariate regression to assess the relationship between biomechanical parameters as dependent variables and the relevant predictive factors such as age, mean keratometry (K), thickness point, sphere, cylinder, and BCVA as independent variables. Each variable ($P < 0.2$) was used in multivariate regression analysis to assess the final relationship between biomechanical parameters and the relevant predictive factors. We used an index for the normal eye from Tian *et al*. articles and used MdCalc online to compare normal and KCN eyes.[26,27]

All statistical analyses were performed using the IBM SPSS software for Windows version 25.0 (IBM Corp. Armonk, NY, USA). All tests were two sided, and $P < 0.05$ was considered statistically significant. All assumptions of the linear regression were considered for statistical analysis based on the forward stepwise selection method.

Results

The mean (±SD) age of patients was 36 ± 3 years, and 36.4% were male [Table 2]. The mean efficacy index was 1.73 with SD 0.92 and the mean safety index was 0.74 with SD 0.49 that both were reported in the study.

All patients were matched for age, intraocular pressure (IOP), and central corneal thickness (CCT). At baseline and latest follow-up, the averages of the mean spherical equivalent were −13.48 ± 2.86 D and −8.59 ± 2.17 D ($P < 0.007$) and mean keratometry were 54.68 ± 2.77 D and 51.95 ± 2.21 D ($P < 0.006$). According to Corvis ST, the increase in first applanation time (A1T, $P < 0.001$), HC time (HCT, $P = 0.004$), radius ($P < 0.001$), peak distance during HC state (PD, $P = 0.018$), Ambrósio's relational thickness to the horizontal profile (ARTh, $P < 0.001$), first applanation stiffness parameter (SP-A1, $P < 0.001$), and CCT ($P < 0.001$) were statistically significant after lenticule implantation; the decrease in first applanation velocity (A1V, $P < 0.001$), first

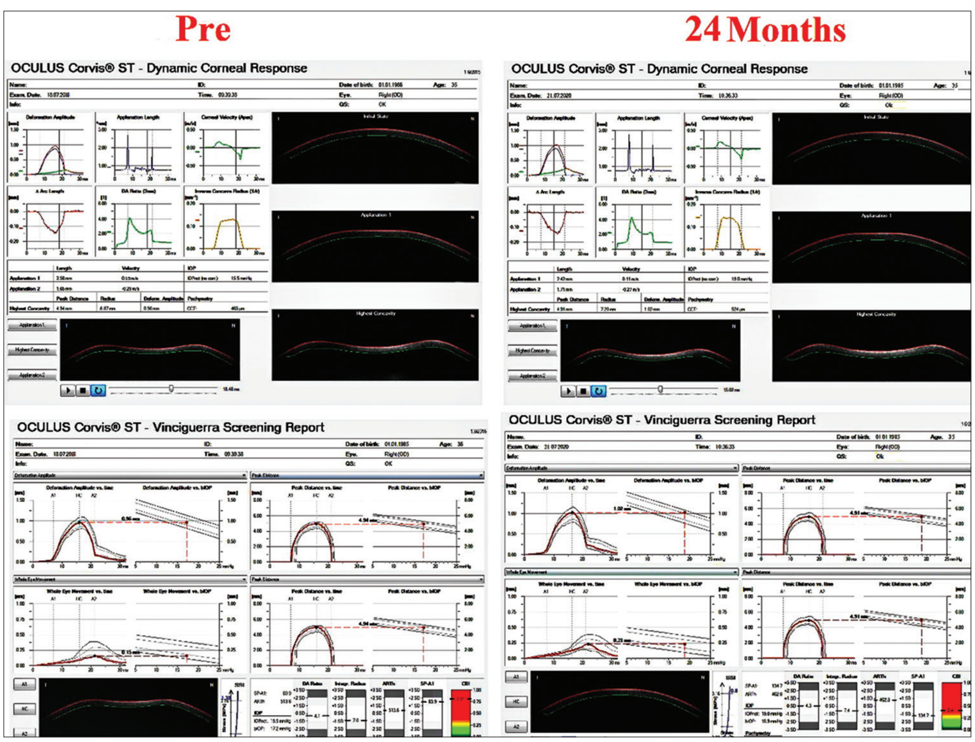

Figure 3: Corvis ST overview display

Table 1: Corvis ST - parameters

Parameters	Abbreviation	Description
Biomechanically corrected intraocular pressure	bIOP	Derived by finite element simulations that take into account the influence of central corneal thickness, age, and DCR parameters
First applanation A1	A1	The moment at the first applanation of the cornea during the air puff
A1 time (ms)	A1T (T1)	Time from start to A1
A1 velocity (m/s)	A1V (V1)	Velocity (speed) of corneal apex at A1
A1 deformation amplitude	A1DA	Moving distance of the corneal apex from the initial position to that at the A1 time
A1 deflection length	A1DL	Length of the flattened cornea at A1
A1 deflection amplitude	A1DeflA A1DLA	After approaching the highest displacement secondary to WEM, the whole eye displays a nonlinear motion in the ant-post direction. Hence, A1DeflA is similar to A1DA without WEM
A1 delta arc length	A1dArclength A1dArcL	Change in arc length from the initial state to A1, in a defined 7 mm zone
Second applanation A2	A2	The moment at the first applanation of the cornea during the air puff
A2 time (ms)	A2T (T2)	Time from start to A2
A2 velocity (m/s)	A2V	Speed of corneal apex at A2
A2 deformation amplitude	A2DA	Moving the distance of the corneal apex from the initial position to that at A2 time
A2 deflection length	A2DL	Length of the flattened cornea at A2
A2 deflection amplitude	A2DeflA A2DLA	Similar to A2DA without whole eye movement
A2 delta arc length	A2dArclength A2dArcL	Change in arc length from the initial state to A2, in a defined 7 mm zone
Highest (maximum) concavity	HC, MC	The moment that the cornea assumes its maximum concavity during the air puff
HC time	HCT	Time to reach the maximum deformation
Radius (mm)	Rad	Central curvature radius at the HC state secondary to parabolic fit
HC (maximum) deformation amplitude	HCDA, MDA	Maximum depth of ant-post corneal displacement at the moment of maximum concavity
HC deflection length	HCDL	Length of the flattened cornea at the highest concavity
HC deflection amplitude	HCDeflA, HCDLA	The “displaced” area of the cornea in the horizontal plane secondary to corneal deformation
Peak distance	PD	Distance between the two peaks of the cornea in the temporal-nasal direction at the maximum concavity state, which is not the same as the deflection length
HC delta Arc length	HCdArclength	Change in arc length in a defined 7 mm zone during HC from the initial state
Maximum	Max	Similar to HC
Maximum deformation amplitude	Max DA	The distance of the corneal apex movement from the initiation of the deformation to the HC
Maximum deflection amplitude	Max DeflA	The ratio between the deformation/deflection amplitude at the apex and the average deformation/deflection amplitude in a nasal and temporal zone 1 or 2 mm (2 mm for DefA ratio) from the center. Higher values (greater 1) of DA Ratio and DefA Ratio can be associated with less resistant corneas
Maximum delta arc length	MaxdArclength	Change in arc length during the highest concavity moment from the initial state, in a 7 mm with horizontal direction (3.5 mm from the apex to both sides)
VSP		
Deformation amplitude ratio max (2 mm)	DA ratio max (DAR 2 mm)	The ratio between the deformation amplitude at the apex and the average deformation amplitude measured at 2 mm central-peripheral
Ambrósio’s relational thickness to the horizontal profile	ARTh	The ratio between the deformation amplitude at the apex and the average deformation amplitude measured at 2 mm from the center
Integrated radius	INR (IR)	Area under the inverse concave radius versus time curve. In fact, 1/R is plotted during the time of an air pulse is entirely measured between the period of first and second applanation
Stiffness parameter at A1	SP-A1	Corneal stiffness at A1, the ratio of resultant pressure to deflection amplitude
Corvis biomechanical index	CBI	Overall biomechanical index for keratoconus detection

DCR=Dynamic corneal response, 1/R=The inverse concave radius, WEM=Whole eye globe movement, Ant-Post=Anterior-posterior, VSP=Vinciguerra screening parameters

applanation deflection amplitude (A1DeflA, $P = 0.055$), second applanation deformation amplitude (A2DA, $P = 0.004$), HC deformation amplitude ($P < 0.001$), maximum deformation amplitude ratio (DAR) at 2 mm (DA ratio max, $P < 0.001$), integrated radius (IR, $P = 0.002$), and (CBI, $P < 0.001$) were statistically significant after lenticule implantation [Table 3]. Measurements of Corvis ST are presented in Table 3 and Figure 3.

Stepwise regression

Univariate linear regression was performed to study the relationship between age, sphere, cylinder, mean K, BCVA, and CCT from the 6th month with corneal

Table 2: Demographic data of participants

	Mean±SD	Median	Minimum	Maximum
Age	36.14±2.78	36.00	33.00	42.00
Mean.K.Pre	54.68±2.77	55.00	50.00	59.00
Thickness.CCT.Pre	388.64±34.55	395.00	300.00	455.00
Thickness point.Pre	383.64±42.83	395.00	270.00	455.00
Sph.Pre	−8.48±2.86	−8.00	−15.00	−5.00
Cylinder.Pre	−8.23±1.59	−8.50	−11.00	−5.00
BCAV.Pre	0.70±0.17	0.70	0.40	1.00
Sex, *n* (%)	Male: 8 (36.4)		Female: 14 (63.6)	

K mean=Mean keratometry, BCVA=Best corrected visual acuity, SD=Standard deviation, CCT=Central corneal thickness

biomechanical factors [Table 4] and using the data from the multivariate regression analysis.

Then, the stepwise multivariable regression study found that age was positively correlated with SP-A1 (P = 0.003) and negatively correlated with HC delta Arc length (HCdArcL; P = 0.007). The sphere was positively correlated with HCT (P = 0.036) and negatively correlated with HCdAarcL (P = 0.003). Mean K was positively correlated with CCT (P = 0.05) and negatively associated with CBI (P = 0.032). BCVA was positively correlated with HCT (P = 0.044). The cylinder was positively correlated with PD (P = 0.05) and CCT (P = 0.05), whereas it was negatively correlated with IR (P = 0.025) [Table 5].

Both the max deformation amplitude (MDA) and CBI had a high Youden index (0.86 and 0.82, respectively). MDA showed a cutoff value of 1.1 and 88.36% sensitivity, 100% specificity, and area under the curve (AUC) 0.962 ± 0.027 (95% confidence interval [CI]: 0.909–1; P < 0.001). CBI showed a cutoff of 0.61 and 90.91% sensitivity, 90.91% specificity, and AUC 0.067 ± 0.038 (95% CI: 0–0.142; P < 0.001).

Discussion

Corneal biomechanical evaluation using the Corvis ST illustrated statistically significant differences 6 months after lenticule implantation in several parameters that remained stable over 2 years of follow-up. The established Corvis ST parameters of the eyes in the current study are presented in Table 1 and Figure 3. Table 3 shows the distribution and changes in the Corvis ST parameters between the two groups.

Among the standard corneal resistance parameters, V1 and the maximum radius changed significantly after lenticule implantation (P < 0.001). A significant increase in CCT and SP-A1 and a considerable decrease in IR and DAR indicated an increase in corneal stiffness. The difference between pre and postoperative IOP assessed using the Corvis ST was not significant.

Clinical studies with long-term follow-up support the effectiveness of stromal augmentation for KCN. These previous studies have shown an improvement in uncorrected and best spectacle-corrected visual acuity, confocal scan, optical coherence tomography, pachymetric, and topometric indices such as index height asymmetry = 3.6 and central KCN index = 1.04.[18,19,28] The new Corvis ST parameters of the normal and postoperative groups are shown in Figure 4. Thus, changes in corneal biomechanics in KCN eyes might be converted through lenticule implantation with thickness more than 100 μ according to Figure 1, even in corneas thinner than 400, which creates a dilemma for CXL to halt KCN progression.

To our knowledge, this is the first study to report biomechanical indices of the cornea after stromal augmentation by lenticule implantation.

Contradictory to all previous studies which had indicated the reduction of corneal thickness after CXL, probably secondary to artifacts of multiple scattering in the corneal stroma;[6,9,10,29,30] we observed an increase in CCT and corneal pachymetry at the thinnest point as expected. Corneal stiffness in KCN has been reported to be approximately 60% of that in the normal cornea.[10] This has been attributed to differences in collagen bonding patterns.

Moreover, according to previous reports, Alió *et al*.,[31-34] Yang *et al*.,[35] and the results of the current study, it can be suggested that lenticule implantation with a thickness of more than 100 μ according to Figure 1 is characterized by an augmentation of material properties that lead to progressive thickening, bonding, decreasing strain, stress redistribution, and further keratocyte densities. During CXL, the posterior stroma is mainly unchanged due to nearly 70% of UV-A radiation absorption in the anterior third. This may have contributed to these dissimilarities.[6,8,10,26,29,35,36]

Limitations of the study

One of our study's limitations was the relatively small sample size, which means that despite a long-term follow-up for valid conclusions and elimination of irrelevancy during an extended period, a multicenter study and a control or sham group as a comparison could assist in more accurate and reliable evaluations. Furthermore, subtle changes in corneal biomechanics may be neglected by an extended area, which is attributed to the ocular response analyzer (ORA) and even Corvis ST measurements.[10] In this respect, unchanged data after any intervention may be attributed to the lack of better predictors[27] of corneal biomechanics such as SP-A1, Deformation amplitude ratio max (DARM), IR, and CBI after stromal augmentation. Moreover, none of

Table 3: Comparison of Corvis ST parameters between measurements obtained before and after stromal lenticule implantation

Variables	Mean±SD Median (range), *P* value within			
	Base (KC eyes)	3 months	6 months	24 months
A1T (m/s)	6.5±0.26	6.61±0.35	7.09±0.3	7.19±0.22
	6.46 (6.12–6.9)	6.75 (5.8–7.1), 0.167	7.15 (6.4–7.6), <0.001	7.25 (6.8–7.5), <0.001
A1V (m/s)	0.16±0.02	0.14±0.02	0.13±0.02	0.13±0.02
	0.17 (0.12–0.2)	0.14 (0.11–0.19), 0.002	0.13 (0.11–0.18), <0.001	0.12 (0.1–0.17), <0.001
A1DA	0.12±0.01	0.11±0.01	0.11±0.01	0.11±0.02
	0.12 (0.09–0.14)	0.11 (0.09–0.13), 0.184	0.11 (0.09–0.13), 0.086	0.11 (0.09–0.13), 0.1
A1DL	2.15±0.16	2.15±0.17	2.14±0.14	2.14±0.18
	2.15 (1.9–2.4)	2.12 (1.9–2.4), 0.896	2.13 (1.9–2.4), 0.817	2.11 (1.9–2.4), 0.741
A1DeflA	0.08±0.01	0.07±0.02	0.07±0.03	0.07±0.02
	0.09 (0.06–0.1)	0.08 (0.01–0.1), 0.143	0.07 (0.01–0.1), 0.051	0.08 (0.01–0.1), 0.055
A1dArcL	−0.01±0	−0.01±0	−0.01±0	−0.01±0
	−0.02 (−0.02–−0.01)	−0.01 (−0.02–−0.01), 0.503	−0.02 (−0.02–−0.01), 0.849	−0.01 (−0.02–−0.01), 0.505
A2T (ms)	22.12±1.07	22.06±0.94	21.66±1	21.57±1.19
	21.72 (20.71–23.99)	21.79 (20.71–23.95), 0.861	22 (19–23.02), 0.181	21.6 (19–23.88), 0.146
A2V (m/s)	−0.46±0.16–0.4(−0.83–−0.22)	−0.45±0.14–0.44 (−0.83–−0.22), 0.808	−0.43±0.16–0.39 (−0.83, −0.24), 0.546	−0.43±0.15–0.38 (−0.75, −0.22), 0.461
A2DA	0.34±0.04	0.31±0.05	0.31±0.04	0.3±0.03
	0.35 (0.28–0.41)	0.31 (0.23–0.4), 0.001	0.3 (0.23–0.39), 0.016	0.3 (0.23–0.39), 0.004
A2DL	3.01±0.36	3.04±0.29	3.02±0.23	3.08±0.29
	3.05 (2–3.9)	3 (2.2–3.8), 0.785	3 (2.3–3.5), 0.936	3.1 (2.3–3.9), 0.446
A2DeflA	0.1±0.02	0.1±0.01	0.1±0.01	0.1±0.01
	0.1 (0.05–0.15)	0.1 (0.07–0.12), 0.502	0.1 (0.08–0.12), 0.874	0.1 (0.08–0.12), 0.861
A2dArcL	−0.02±0.01–0.02 (−0.07–−0.01)	−0.02±0	−0.02±0	−0.02±0
		−0.02 (−0.03–−0.01), 0.513	−0.02 (−0.03–−0.01), 0.355	−0.02 (−0.03–−0.01), 0.545
HCT	15.29±1.47	16.21±1.39	16.61±1.5	16.8±1.71
	15.31 (12.11–17.5)	16.37 (13.32–19), 0.068	16.88 (12.25–19.2), 0.004	16.85 (12.25–19.5), 0.004
Rad	5.86±0.50	6.76±0.38	6.82±0.43	7±0.39
	5.9 (5.02–6.8)	6.86 (6.02–7.3), <0.001	6.9 (6.02–7.5), <0.001	7.02 (6.08–7.54), <0.001
MDA	1.24±0.14	1±0.07	0.98±0.05	1.01±0.06
	1.24 (1–1.5)	1 (0.89–1.12), <0.001	0.99 (0.89–1.08), <0.001	1 (0.89–1.12), <0.001
HCDL	5.39±0.32	5.42±0.35	5.4±0.32	5.42±0.31
	5.41 (4.8–6)	5.41 (4.8–6), 0.797	5.4 (4.8–6), 0.937	5.41 (4.8–6), 0.823
HCDeflA	0.97±0.08	0.95±0.08	0.94±0.08	0.94±0.08
	0.98 (0.85–1.1)	0.97 (0.8–1.1), 0.543	0.96 (0.8–1.08), 0.152	0.97 (0.8–1.08), 0.274
PD	4.49±0.37	4.6±0.33	4.68±0.27	4.73±0.27
	4.48 (3.9–5.2)	4.6 (4.1–5.2), 0.246	4.69 (4.05–5.2), 0.077	4.75 (4.1–5.2), 0.018
HCdArcL	−0.12±0.03–0.11 (−0.21–0.09)	−0.12±0.02–0.12 (−0.15–0.09), 0.645	−0.12±0.02–0.11 (−0.15–0.09), 0.44	−0.12±0.02–0.11 (−0.15–−0.09), 0.515
DARM	6.25±0.37	5.99±0.4	5.7±0.69	5.6±0.69
	6.23 (5.42–6.9)	6 (5.02–6.7), <0.001	5.9 (4.2–6.7), 0.003	5.85 (4.2–6.7), <0.001
ARTh	301.64±78.15	487.27±46.73	483.27±47.32	488.86±37.35
	300 (230–450)	495.5 (350–550), <0.001	502 (345–542), <0.001	500 (380–530), <0.001
bIOP	14.32±1.59	14±1.54	14.23±1.8	14.14±1.49
	14 (12–17)	14 (12–18), 0.245	14 (12–18), 0.851	14 (12–17), 0.669
IR	12.55±2.3	12.11±2.31	11.02±2.12	10.05±2.09
	12 (9–17)	12.5 (9–16.5), 0.038	10 (8.9–16.5), 0.051	10 (6.9–15), 0.002
SP-A1	66.77±13.28	74.64±19.1	99.27±12.64	100.27±11.42
	65 (45–98)	75 (45–114), 0.107	95 (81–125), <0.001	98.5 (85–125), <0.001
CCT	388.64±34.55	494.23±35.76	477.18±42.21	475.55±41.32
	395 (300–455)	500 (410–542), <0.001	489.5 (380–526), <0.001	487 (380–521), <0.001

Contd...

Table 3: Contd...

Variables	Mean±SD Median (range), *P* value within			
	Base (KC eyes)	3 months	6 months	24 months
CBI	0.83±0.15	0.61±0.16	0.4±0.18	0.3±0.14
	0.87 (0.55–1)	0.6 (0.3–0.8), <0.001	0.4 (0.1–0.7), <0.001	0.3 (0.1–0.6), <0.001

The parameters of first (A1) and second (A2) applications, The parameters of HC and VSP. A1T=A1 time, A1V=A1 velocity, A1DA=A1 deformation amplitude, A1DL=A1 deflection length, A1DeflA=A1 deflection amplitude, A1dArcL=A1 delta arc length, A2T=A2 time, A2V=A2 velocity, A2DA=A2 deformation amplitude, A2DL=A2 deflection length, A2DeflA=A2 deflection amplitude, A2dArcL=A2 delta arc length, HC=Highest (maximum) concavity, VSP=Vinciguerra screening parameter, HCT=HC time, Rad=Radius, MDA=Maximum deformation amplitude, HCDL=HC deflection length, HCDeflA=HC deflection amplitude, PD=Peak distance, HCdArcL=HC delta arc length, DARM=Deformation amplitude ratio, ARTh=Ambrósio's relational thickness to the horizontal profile, bIOP=Biomechanically corrected intraocular pressure, IR=Integrated radius, SP-A1=Stiffness parameter at A1, CCT=Central corneal thickness, CBI=Corvis biomechanical index, SD=Standard deviation, KCN=Keratoconus

Table 4: The results of the univariate linear regression model after 6 months

	Age		Mean K		Thickness of thinnest point		Sphere		Cylinder		BCVA	
	β	*P*	β	*P*	β	*P*	β	*P*	β	*P*	β	*P*
A1T	−0.071	0.753	−0.299	0.176	−0.036	0.874	0.023	0.921	−0.179	0.424	−0.056	0.803
A1V	−0.265	0.233	0.282	0.204	0.166	0.459	0.115	0.609	0.049	0.828	−0.083	0.714
A1DA	0.134	0.551	0.084	0.711	−0.051	0.821	−0.404	0.062	−0.037	0.870	0.041	0.857
A1DL	0.241	0.279	0.215	0.336	0.091	0.687	−0.052	0.817	−0.009	0.970	0.114	0.613
A1DeflA	0.137	0.544	0.055	0.807	0.260	0.242	−0.061	0.789	0.120	0.594	−0.090	0.690
A1dArcL	−0.359	0.101	0.011	0.961	0.061	0.786	−0.327	0.138	−0.050	0.825	0.187	0.406
A2T	0.268	0.227	−0.210	0.349	−0.039	0.864	0.278	0.211	−0.063	0.780	−0.029	0.899
A2V	0.005	0.981	0.275	0.216	−0.259	0.244	−0.290	0.191	−0.288	0.194	−0.048	0.833
A2DA	0.021	0.927	−0.117	0.605	−0.174	0.438	−0.067	0.766	0.074	0.742	−0.387	0.075
A2DL	0.053	0.814	−0.017	0.939	−0.239	0.285	−0.062	0.785	−0.212	0.343	0.108	0.634
A2DeflA	−0.164	0.467	0.059	0.795	0.331	0.132	−0.265	0.233	−0.044	0.844	−0.105	0.643
A2dArcL	0.163	0.469	0.233	0.296	0.039	0.865	0.187	0.404	0.096	0.672	−0.195	0.384
HCT	−0.149	0.509	0.146	0.516	0.282	0.204	0.478	0.024	−0.173	0.441	0.463	0.030
Radius	−0.057	0.801	0.148	0.512	0.241	0.280	0.000	1.000	0.045	0.843	0.106	0.638
HCDA	−0.163	0.468	−0.098	0.663	−0.036	0.873	−0.074	0.745	−0.026	0.908	−0.070	0.757
HCDL	−0.043	0.850	0.353	0.107	0.190	0.398	0.137	0.543	0.066	0.771	0.089	0.695
HCDeflA	0.143	0.525	0.111	0.621	0.021	0.926	0.198	0.378	0.060	0.790	0.080	0.722
PD	−0.024	0.916	−0.266	0.231	−0.156	0.489	0.107	0.636	0.418	0.053	−0.218	0.330
HCdArcL	−0.518	0.013	0.139	0.537	−0.025	0.912	−0.571	0.006	0.081	0.721	−0.244	0.274
DARM	0.065	0.775	−0.303	0.170	0.024	0.916	0.040	0.860	−0.304	0.170	0.160	0.477
ARTH	0.025	0.912	−0.112	0.619	0.255	0.253	0.195	0.385	0.266	0.232	0.076	0.738
bIOP	−0.140	0.535	0.254	0.254	0.242	0.278	−0.171	0.445	−0.192	0.391	−0.279	0.209
IR	0.151	0.501	0.055	0.809	−0.112	0.619	−0.053	0.815	−0.476	0.025	−0.268	0.227
SP-A1	0.600	0.003	0.138	0.539	−0.019	0.934	0.079	0.726	0.244	0.273	0.103	0.649
CBI	0.060	0.790	−0.458	0.032	−0.237	0.289	0.014	0.950	0.233	0.297	0.057	0.800
CCT	0.009	0.968	0.386	0.076	0.999	0.000	0.134	0.552	0.300	0.174	0.276	0.214

Univariate linear regression analysis. Coefficient (β): Indicates regression coefficient and $P<0.2$ were significant and used in multivariate regression analysis. A1T=A1 time, A1V=A1 velocity, A1DA=A1 deformation amplitude, A1DL=A1 deflection length, A1DeflA=A1 deflection amplitude, A1dArcL=A1 delta arc length, A2T=A2 time, A2V=A2 velocity, A2DA=A2 deformation amplitude, A2DL=A2 deflection length, A2DeflA=A2 deflection amplitude, A2dArcL=A2 delta arc length, HC=Highest (maximum) concavity, HCT=HC time, HCDA=HC deformation amplitude, HCDL=HC deflection length, HCDeflA=HC deflection amplitude, PD=Peak distance, HCdArcL=HC delta arc length, DARM=Deformation amplitude ratio, ARTh=Ambrósio's relational thickness to the horizontal profile, bIOP=Biomechanically corrected intraocular pressure, IR=Integrated radius, SP-A1=Stiffness parameter at A1, CCT=Central corneal thickness, CBI=Corvis biomechanical index, Mean K=Mean keratometry, BCVA=Best-corrected visual acuity

the devices considered the volume pressure originating from the fluid in the anterior chamber.

Strengths of the study

The strengths of the current study are the lack of any effect of eye drops that can affect corneal biomechanical properties,[37] the evaluation of all corneal biomechanical indices by Corvis ST as better predictors[38] of corneal biomechanics such as SP-A1, DARM, IR, CCT, and CBI, and their close relationship with ORA measured corneal hysteresis and corneal resistance factor.[39,40]

In the multivariate stepwise linear regression analysis model, age was significantly and negatively correlated with HCdArcL and DARM and positively correlated with SP-A1, similar to a previous study (positive correlation with KCN). The biomechanical indices and corneal tomographic parameters in patients with KCN have been defined in previous studies.[41,42] In the current study,

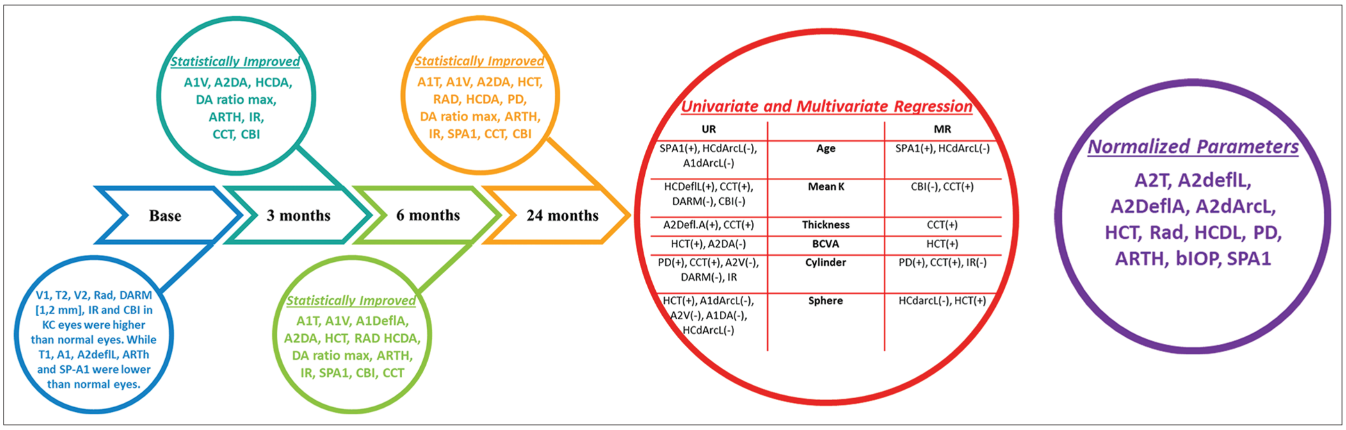

Figure 4: The established parameters that presented significant differences with the normal population, among preoperatively (keratoconus eyes) and postoperatively (eyes with lenticules) and during three courses of follow-up and correlated parameters (from left to right, respectively). HCDA = Highest concavity deformation amplitude, DA Ratio Max = Maximum deformation amplitude ratio, ARTH = Ambrósio's relational thickness, IR = Integrated radius, CBI = Corvis biomechanical index, CCT = Central corneal thickness, HCT = Highest concavity time, RAD = Radius, PD = Peak distance

Table 5: The results of the multivariate regression model after 6 months

	Age		Mean K		Thickness point		Sphere		Cylinder		BCVA	
	β	*P*	β	*P*	β	*P*	β	*P*	β	*P*	β	*P*
HCT							0.38	0.036			4.964	0.044
PD									0.418	0.05		
HCdArcL	−0.003	0.007					−0.006	0.003				
IR									−0.476	0.025		
SP-A1	0.600	0.003										
CBI			−0.458	0.032								
CCT			0.386	0.05	1.014	<0.001			1.04	0.05		

Coefficient (β): Indicates regression coefficient and $P<0.05$ indicates statistically significant. HC=Highest (maximum) concavity, HCT=HC time, PD=Peak distance, HCdArcL=HC delta arc length, IR=Integrated radius, SP-A1=Stiffness parameter at A1, CCT=Central corneal thickness, CBI=Corvis biomechanical index, Mean K=Mean keratometry, BCVA=Best-corrected visual acuity

the mean keratometry value (Km) was statistically and positively associated with CCT. A negative correlation was found with CBI in both regressions, and CCT was statistically and positively correlated with A2defA.

Similar to the study by Fujishiro *et al.*,[39] CCT was significantly related to all of the Corvis ST indexes; thick CCT was related considerably to low DAR (flat cornea around the corneal apex at the HCT), high ARTh (thick, thinnest point rather than to corneal thickness in the periphery), low CBI (unlikely to be KCN), and large IR (flat corneal deformation close to the corneal apex).

In this study, the negative association of IR with thickness at the thinnest point was probably due to the influence of the original shape of the cornea (curvature). ARTh = CT thinnest/pachymetric progression is the quotient of corneal thickness at the thinnest point of the horizontal meridian and the thickness changes, and hence it has a positive relationship with CCT [Table 3]; hence, the lower index displayed a faster progression of thickness toward the periphery or a thinner cornea. A high DA ratio before the augmentation procedure suggests a soft cornea due to the start of corneal deformation at the center of the cornea.[39] The stiff cornea (high SP-A1: the difference between the strength of the air puff at the corneal surface) is resistant postoperatively.

The value of CBI is based on a logistic regression formula calculated from different Corvis ST parameters (A1V, ARTh, SP-A1, DA ratio max [2 mm], DA ratio max [1 mm], and Deflection amplitude (DLA). It displays a capacity for ectasia progression as follows: values between 0.25 and 0.5 indicate a moderate risk, <0.25 and >0.5 indicate a low and high risk of developing ectasia, respectively.[39,41] In the current study, the CBI values between eyes with lenticules and KCN eyes were significantly different, which indicated that the value of CBI could be used to differentiate the rate of efficacy.

Notwithstanding, clinicians should be cautious when interpreting Corvis ST results for several reasons. On one hand, evidence for KCN staging according to Corvis ST was either poor[29] or presented different cutoff values of tomographic and biomechanical index (TBI = 0.29)[38,42-44] and in combination with CBI (TBI = 0.49, CBI = 0.78).[9] On the other hand, different methodologies and follow-up periods have led to a lack of consistent results observed in studies. Furthermore, heterogeneous biomechanical properties of KCN corneas, for instance, an increase in the corneal stiffness over age,[10] reduction in corneal stiffness after phacoemulsification surgery,[45] or Visian V4c implantation and stabilization after 3 months.[46] Finally, since in the lenticule implantation, the Descemet's membrane is preserved, based on expectation,[35,46-50] biomechanical outcomes are nearer to deep anterior lamellar keratoplasty than penetrating keratoplasty. Nevertheless, differences between keratoplasty indications or graft-related items may explain the contradictory results[47] [Table 4].

Conclusions

This research provides a full understanding of the clinical problems that must be overcome to make the best decisions possible in the treatment of KCN.

We shall soon see the adoption of spatially resolved *in vivo* corneal biomechanical evaluation, which will complement traditional geometrical evaluation and open the way for tailored therapy.

Our study shows the efficacy of regenerative treatment in KCN on keratometric stability and visual acuity after a 2-year follow-up, highlighting an interesting field of research that offers the possibility to address disease pathology at the cellular level. The *in vivo* observations with Corvis ST in KCN cases illustrated that stromal augmentation induces significant effects on corneal biomechanical properties; the predictive accuracy of stromal augmentation needs to be elucidated in future studies.

Acknowledgments
We would like to thank Editage (www.editage.com) for English language editing.

Financial support and sponsorship
This study was supported in part by the Red Temática de Investigación Cooperativa en Salud, reference number RD16/0008/0012, funded by Instituto de Salud Carlos III and co-funded by the European Regional Development Fund.

Conflicts of interest
Prof. Jorge L. Alio, an international editorial board member at *Taiwan Journal of Ophthalmology*, had no role in the peer review process of or decision to publish this article. The other authors declared no conflicts of interest in writing this paper.

References

1. Vega-Estrada A, Mimouni M, Espla E, Alió Del Barrio J, Alio JL. Corneal epithelial thickness intrasubject repeatability and its relation with visual limitation in keratoconus. Am J Ophthalmol 2019;200:255-62.
2. Niazi S, Jiménez-García M, Findl O, Gatzioufas Z, Doroodgar F, Shahriari MH, *et al.* Keratoconus diagnosis: From fundamentals to artificial intelligence: A systematic narrative review. Diagnostics (Basel) 2023;13:2715.
3. Sachdev GS, Sachdev R, Sachdev MS. Intra corneal ring segment implantation with lenticule assisted stromal augmentation for crosslinking in thin corneas. Am J Ophthalmol Case Rep 2020;19:100726.
4. Hafezi F, Kling S, Gilardoni F, Hafezi N, Hillen M, Abrishamchi R, *et al.* Individualized corneal cross-linking with riboflavin and UV-A in ultrathin corneas: The sub400 protocol. Am J Ophthalmol 2021;224:133-42.
5. Pedrotti E, Chierego C, Bonacci E, De Gregorio A, De Rossi A, Zuliani A, *et al.* New treatments for keratoconus. Int Ophthalmol 2020;40:1619-23.
6. Salouti R, Khalili MR, Zamani M, Ghoreyshi M, Nowroozzadeh MH. Assessment of the changes in corneal biomechanical properties after collagen cross-linking in patients with keratoconus. J Curr Ophthalmol 2019;31:262-7.
7. Garcia-Porta N, Fernandes P, Queiros A, Salgado-Borges J, Parafita-Mato M, González-Méijome JM. Corneal biomechanical properties in different ocular conditions and new measurement techniques. ISRN Ophthalmol 2014;2014:724546.
8. Bamdad S, Sedaghat MR, Yasemi M, Maalhagh M. Intracorneal stromal ring can affect the biomechanics of ectatic cornea. J Ophthalmol 2020;2020:4274037.
9. Sedaghat MR, Momeni-Moghaddam H, Ambrósio R Jr., Heidari HR, Maddah N, Danesh Z, *et al.* Diagnostic ability of corneal shape and biomechanical parameters for detecting frank keratoconus. Cornea 2018;37:1025-34.
10. Jabbarvand M, Moravvej Z, Shahraki K, Hashemian H, Ghasemi H, Berijani S, *et al.* Corneal biomechanical outcome of collagen cross-linking in keratoconic patients evaluated by corvis ST. Eur J Ophthalmol 2021;31:1577-83.
11. Li M, Wei R, Yang W, Shang J, Fu D, Xia F, *et al.* Femtosecond laser-assisted allogenic lenticule implantation for corneal ectasia after LASIK: A 3-year *in vivo* confocal microscopic investigation. J Refract Surg 2020;36:714-22.
12. Fuchsluger TA, Brettl S, Geerling G, Kaisers W, Franko Zeitz P. Biomechanical assessment of healthy and keratoconic corneas (with/without crosslinking) using dynamic ultrahigh-speed Scheimpflug technology and the relevance of the parameter (A1L-A2L). Br J Ophthalmol 2019;103:558-64.
13. Beshtawi IM, O'Donnell C, Radhakrishnan H. Biomechanical properties of corneal tissue after ultraviolet-A-riboflavin crosslinking. J Cataract Refract Surg 2013;39:451-62.
14. Riau AK, Htoon HM, Alió Del Barrio JL, Nubile M, El Zarif M, Mastropasqua L, *et al.* Femtosecond laser-assisted stromal keratophakia for keratoconus: A systemic review and meta-analysis. Int Ophthalmol 2021;41:1965-79.
15. Moshirfar M, Stoakes IM, Bruce EG, Ali A, Payne CJ, Furhiman D, *et al.* Allogenic lenticular implantation for correction of refractive error and ectasia: Narrative review. Ophthalmol Ther 2023;12:2361-79.
16. Hashemi H, Doroodgar F, Niazi S, Khabazkhoob M, Heidari Z. Comparison of different corneal imaging modalities using artificial intelligence for diagnosis of keratoconus: A systematic review and meta-analysis. Graefes Arch Clin Exp Ophthalmol 2023. [doi: 10.1007/s00417-023-06154-6].
17. Niazi S, Moshirfar M, Doroodgar F, Alió Del Barrio JL, Jafarinasab MR, Alió JL. Cutting edge: Corneal stromal lenticule implantation (corneal stromal augmentation) for ectatic disorders. Cornea 2023;42:1469-75.
18. Doroodgar F, Jabbarvand M, Niazi S, Karimian F, Niazi F, Sanginabadi A, *et al.* Customized stromal lenticule implantation for keratoconus. J Refract Surg 2020;36:786-94.
19. Doroodgar F. Outcome simultaneous replacement of stromal donor lenticul in cornea with ectasia during smile surgery. Acta

Ophthalmol 2019;97:S263.
20. Hu X, Wei R, Liu C, Wang Y, Yang D, Sun L, *et al.* Recent advances in small incision lenticule extraction (SMILE)-derived refractive lenticule preservation and clinical reuse. Eng Regen 2023;4:103-121.
21. Liang G, Wang L, Pan Z, Zhang F. Comparison of the different preservative methods for refractive lenticules following SMILE. Curr Eye Res 2019;44:832-9.
22. Nemcokova M, Dite J, Klimesova YM, Netukova M, Studeny P. Preservation of corneal stromal lenticule: Review. Cell Tissue Bank 2022;23:627-39.
23. Rezaei Kanavi M, Ghalenoee M, Chamani T, Javadi M, Fazili N. Comparison of donor cornea storage in Optisol-GS and the central eye bank of Iran (CEBI) Medium. Bina J Ophthalmol 2015;20:374-9.
24. Moshirfar M, Shah TJ, Masud M, Linn SH, Ronquillo Y, Hoopes PC Sr. Surgical options for retreatment after small-incision lenticule extraction: Advantages and disadvantages. J Cataract Refract Surg 2018;44:1384-9.
25. Vinciguerra R, Ambrósio R Jr., Elsheikh A, Roberts CJ, Lopes B, Morenghi E, *et al.* Detection of keratoconus with a new biomechanical index. J Refract Surg 2016;32:803-10.
26. Tian L, Huang YF, Wang LQ, Bai H, Wang Q, Jiang JJ, *et al.* Corneal biomechanical assessment using corneal visualization scheimpflug technology in keratoconic and normal eyes. J Ophthalmol 2014;2014:147516.
27. Kenia VP, Kenia RV, Pirdankar OH. Association between corneal biomechanical parameters and myopic refractive errors in young Indian individuals. Taiwan J Ophthalmol 2020;10:45-53.
28. Jacob S, Patel SR, Agarwal A, Ramalingam A, Saijimol AI, Raj JM. Corneal allogenic intrastromal ring segments (CAIRS) combined with corneal cross-linking for keratoconus. J Refract Surg 2018;34:296-303.
29. Hashemi H, Ambrósio R Jr., Vinciguerra R, Vinciguerra P, Roberts CJ, Ghaffari R, *et al.* Two-year changes in corneal stiffness parameters after accelerated corneal cross-linking. J Biomech 2019;93:209-12.
30. Steinberg J, Siebert M, Katz T, Frings A, Mehlan J, Druchkiv V, *et al.* Tomographic and biomechanical scheimpflug imaging for keratoconus characterization: A validation of current indices. J Refract Surg 2018;34:840-7.
31. Alió JL, Alió Del Barrio JL, El Zarif M, Azaar A, Makdissy N, Khalil C, *et al.* Regenerative surgery of the corneal stroma for advanced keratoconus: 1-year outcomes. Am J Ophthalmol 2019;203:53-68.
32. Alió Del Barrio JL, El Zarif M, Azaar A, Makdissy N, Khalil C, Harb W, *et al.* Corneal stroma enhancement with decellularized stromal laminas with or without stem cell recellularization for advanced keratoconus. Am J Ophthalmol 2018;186:47-58.
33. Alió Del Barrio JL, El Zarif M, de Miguel MP, Azaar A, Makdissy N, Harb W, *et al.* Cellular therapy with human autologous adipose-derived adult stem cells for advanced keratoconus. Cornea 2017;36:952-60.
34. El Zarif M, Alió JL, Alió Del Barrio JL, De Miguel MP, Abdul Jawad K, Makdissy N. Corneal stromal regeneration: A review of human clinical studies in keratoconus treatment. Front Med (Lausanne) 2021;8:650724.
35. Yang K, Xu L, Fan Q, Zhao D, Ren S. Repeatability and comparison of new Corvis ST parameters in normal and keratoconus eyes. Sci Rep 2019;9:15379.
36. Ziaei M, Vellara HR, Gokul A, Ali NQ, McGhee CN, Patel DV. Comparison of corneal biomechanical properties following penetrating keratoplasty and deep anterior lamellar keratoplasty for keratoconus. Clin Exp Ophthalmol 2020;48:174-82.
37. Vinciguerra R, Elsheikh A, Roberts CJ, Ambrósio R Jr., Kang DS, Lopes BT, *et al.* Influence of pachymetry and intraocular pressure on dynamic corneal response parameters in healthy patients. J Refract Surg 2016;32:550-61.
38. Wolffsohn JS, Safeen S, Shah S, Laiquzzaman M. Changes of corneal biomechanics with keratoconus. Cornea 2012;31:849-54.
39. Fujishiro T, Matsuura M, Fujino Y, Murata H, Tokumo K, Nakakura S, *et al.* The relationship between corvis ST tonometry parameters and ocular response analyzer corneal hysteresis. J Glaucoma 2020;29:479-84.
40. Zhang MY, Zhang FJ, Song YZ, Zhao Q, Zhang Y, Yang WL, *et al.* Assessment of corneal biomechanical changes after small incision lenticule extraction with Pentacam and Corvis ST. Zhonghua Yan Ke Za Zhi 2020;56:103-9.
41. Yang K, Xu L, Fan Q, Gu Y, Song P, Zhang B, *et al.* Evaluation of new corvis ST parameters in normal, Post-LASIK, Post-LASIK keratectasia and keratoconus eyes. Sci Rep 2020;10:5676.
42. Koh S, Inoue R, Ambrósio R Jr., Maeda N, Miki A, Nishida K. Correlation between corneal biomechanical indices and the severity of keratoconus. Cornea 2020;39:215-21.
43. Fernández J, Rodríguez-Vallejo M, Piñero DP. Tomographic and biomechanical index (TBI) for screening in laser refractive surgery. J Refract Surg 2019;35:398.
44. Song P, Yang K, Li P, Liu Y, Liang D, Ren S, *et al.* Assessment of corneal pachymetry distribution and morphologic changes in subclinical keratoconus with normal biomechanics. Biomed Res Int 2019;2019:1748579.
45. Wallace HB, Misra SL, Li SS, McKelvie J. Biomechanical changes in the cornea following cataract surgery: A prospective assessment with the corneal visualisation scheimpflug technology. Clin Exp Ophthalmol 2019;47:461-8.
46. Niu L, Miao H, Tian M, Fu D, Wang X, Zhou X. One-year visual outcomes and optical quality of femtosecond laser small incision lenticule extraction and visian implantable collamer lens (ICL V4c) implantation for high myopia. Acta Ophthalmol 2020;98:e662-7.
47. Jafarinasab MR, Feizi S, Javadi MA, Hashemloo A. Graft biomechanical properties after penetrating keratoplasty versus deep anterior lamellar keratoplasty. Curr Eye Res 2011;36:417-21.
48. Blackburn BJ, Jenkins MW, Rollins AM, Dupps WJ. A review of structural and biomechanical changes in the cornea in aging, disease, and photochemical crosslinking. Front Bioeng Biotechnol 2019;7:66.
49. Ryan DS, Coe CD, Howard RS, Edwards JD, Bower KS. Corneal biomechanics following epi-LASIK. J Refract Surg 2011;27:458-64.
50. Doroodgar F, Niazi S. Penetrating keratoplasty versus stromal additional keratoplasty in keratoconus. Invest Ophthalmol Vis Sci 2023;64:2345.